Ionics (2019) 25:2781–2789
https://doi.org/10.1007/s11581-018-2785-y

ORIGINAL PAPER

Preparation of nitrogen and sulfur co-doped graphene aerogel with hierarchical porous structure using ionic liquid precursor for high-performance supercapacitor

Yujuan Chen[1] · Li Sun[1] · Zhiwei Lu[1] · Zhaoen Liu[1] · Yuyang Jiang[1] · Kelei Zhuo[1]

Received: 21 September 2018 / Revised: 17 October 2018 / Accepted: 31 October 2018 / Published online: 11 November 2018

Abstract

In this paper, nitrogen and sulfur co-doped graphene aerogel (NS-GA) was successfully prepared using ionic liquid 1-(4-mercaptobutyl)-3-methylimidazolium bromide (HS-BMIMBr) as both reductant and dopant by a one-step hydrothermal method. The results of X-ray diffraction indicate that the doping of heteroatoms into graphene increases its degree of defects. In addition, scanning electron microscopy measurements and nitrogen adsorption–desorption analysis reveal that the as-prepared NS-GA has unique hierarchical porous nanostructures, which supply efficient networks for ionic transports and electron transfer. The symmetric electrical double-layer capacitors (EDLCs) based on the NS-GA with ionic liquid (1-ethyl-3-methylimidazolium tetrafluoroborate, $EMIMBF_4$) as the electrolyte show excellent capacitive performance. And the NS-GA has a high specific capacitance of 182.3 F g^{-1} at a current density of 1 A g^{-1}. Moreover, there is a high energy density of 101 Wh kg^{-1} at a power density of 1 kW kg^{-1}. Therefore, the NS-GA can be considered as a favorable electrode material for high-performance energy storage devices.

Keywords Nitrogen and sulfur co-doped · Ionic liquid · Hierarchical porous structure · Supercapacitor

Introduction

As a rising star in energy storage field, the supercapacitor has been the focus of both scientific research and industry because of short charging time, high power density, long durability, and high stability feature [1–3]. Electrical double-layer capacitors (EDLCs), which store charges via electrostatic adsorption of the ions between the electrode/electrolyte interfaces, are one of the most widely used supercapacitors [4]. However, EDLCs own lower energy density than batteries, which limits their use in applications [5, 6]. Based on the equation of $E = 1/2\ CV^2$, the effective methods to improve the energy density of EDLCs are to enhance the specific capacitance of the electrode and to widen the range of operating voltage window.

Carbon materials are the most widely used electrode materials to store ions by electrostatic interaction because of their low cost and wide sources. Graphene with a large theoretical specific surface area (2675 $m^2\ g^{-1}$), light weight, high electrical conductivity/mechanical strength, and good stability is a superior carbon material for supercapacitors [7–10]. In order to promote the transport rate of charges/ions between the electrode materials and the electrolyte, researchers further transferred the two-dimensional graphene oxide into porous three-dimensional graphene nanostructures [11]. Graphene aerogels (GAs) are a kind of three-dimensional porous graphene materials with special structure [12]. It is generally accepted that pores are crucial for strengthening the capacitive performance of EDLCs [13, 14]. The heteroatom-doping can improve the wettability of the materials' surface, and thus increase the accessibility of pores [15–17]. The heteroatoms' co-doping can enhance the overall performance of the materials because of the synergetic effect between them. Therefore, more and more efforts have been devoted to the study of heteroatom co-doped in recent years [18–20]. Ionic liquids (ILs), which are known for their unparalleled benign features, such as excellent electrochemical/thermal stability, and high safety, are the most attractive precursors containing heteroatoms [21]. ILs have been introduced into the field of energy equipment as precursors of electrode materials [22].

Another strategy to improve capacitance performance is to use the electrolyte with a wide range of working voltage.

✉ Kelei Zhuo
klzhuo@263.net

[1] Collaborative Innovation Center of Henan Province for Green Manufacturing of Fine Chemicals, Key Laboratory of Green Chemical Media and Reactions, Ministry of Education, School of Chemistry and Chemical Engineering, Henan Normal University, Xinxiang 453007, Henan, People's Republic of China

Frequently used electrolytes include aqueous electrolytes, organic electrolytes, and ILs electrolytes [23]. Aqueous electrolytes are the most frequently used electrolytes because they are low cost and environment-friendly. However, the energy density of supercapacitors is extremely limited by their narrow operating voltage. Organic electrolytes can provide a relatively wide working voltage, but they are flammable and poisonous [24]. Compared with the above two kinds of electrolytes, ILs have been considered as promising candidates in decades due to their wide voltage window and high ionic conductivity. 1-Ethyl-3-methylimidazolium tetrafluoroborate ($EMIMBF_4$) has a relatively wide electrochemical window, low viscosity, high electrical conductivity, and electrochemical stability, and thus is a hopeful electrolyte for fabricating high-performance supercapacitors [25]. However, ILs have a large ionic size which suppresses ion transportation at a high current density [26]. Therefore, porous carbon materials with more accessible channels for ions are benefit to satisfy the demand.

Hence, we prepared a nitrogen and sulfur co-doped graphene aerogel (NS-GA) using a reducing ionic liquid (1-(4-mercaptobutyl)-3-methylimidazolium bromide, HS-BMIMBr) by a fast one-step hydrothermal method. The hydrophilic ionic liquid cannot only improve surface infiltration of graphene materials but also provide heteroatoms. The as-prepared NS-GA reveals an interconnected hierarchical porous structure, which can provide a large accessible channel for the diffusion of electrolyte ions. Additionally, the NS-GA as the electrode material of supercapacitors shows a high specific capacitance of 182.3 F g^{-1} at 1 A g^{-1} in $EMIMBF_4$ electrolyte within a voltage range of 0–4 V. Moreover, the NS-GA presents a high energy density of 101 Wh kg^{-1} at a power density of 1 kW kg^{-1} at a current density of 1 A g^{-1}.

Experiments

Chemicals

1-Methylimidazole (99%), potassium thioacetate (98%), magnesium sulfate (AR), potassium persulfate (99%), graphite powder (99.95%), and hydrogen peroxide (30%) were obtained from Aladdin Industrial Corporation, China. 1-Bromo-4-chlorobutane (98%) was purchased from Shanghai Macklin Biochemical Corporation, China. Acetonitrile (AR), ethyl acetate (AR), dichloromethane (AR), and ethyl alcohol absolute (AR) were purchased from Sinopharm Chemical Reagent Co., Ltd., China. Trichloromethane (AR), potassium permanganate (AR), and concentrated sulfuric acid (AR) were obtained from Luoyang Chem. Co., China. Hydrobromic acid (AR), sodium hydroxide (AR), and phosphorus pentoxide (AR) were purchased from Tianjin Chem. Co., China. $EMIMBF_4$ (99%) was obtained from Lanzhou Institute of Physical Chemistry, Chinese Academy of Sciences, China.

Materials preparation

Graphene oxide (GO) was synthesized from natural graphite powder by the modified Hummers method [27, 28]. The ionic liquid (HS-BMIMBr) was synthesized using the method as described in previous reports with some modification [29, 30]. The NS-GA was synthetized by a simple hydrothermal process (Scheme 1). Briefly, 0.6 g of HS-BMIMBr was added into a GO dispersion (1 mg mL^{-1}, 60 mL). Then, the suspension was transferred to a Teflon-lined autoclave and heated at 200 °C for 4 h. The product was then naturally cooled down to room temperature to obtain N and S co-doped graphene hydrogel (NS-GH). And then the hydrogel was washed several times with deionized (DI) water and dialyzed in DI water for 7 days, where DI water was renewed once a day to remove some impurities. Finally, the hydrogel was freeze-dried for 48 h to obtain the N and S co-doped graphene aerogel, which is denoted as NS-GA. For comparison, graphene aerogel (GA) was also prepared at the same experiment condition without HS-BMIMBr.

Structure characterization

The chemical structure of the materials was characterized by X-ray photoelectron spectroscopy (XPS, Thermo Fisher Scientific, ESCALAB250Xi). The morphologies and microstructures of the samples were characterized by transmission electron microscopy (TEM, JEOL, JEM-2100) and field emission scanning electron microscopy (FESEM, Zeiss, Supra 40). The crystal structures of the samples were measured using X-ray diffractometer (XRD, Bruker, D8 Advance) with Cu-Kα radiation ($\lambda = 0.154$ nm). Raman spectra were obtained by a Raman spectrometer (Renishaw, in-Via) with a 514-nm excitation laser. N_2 adsorption–desorption isotherms were analyzed by nitrogen sorption (Micromeritics, ASAP-2020). The specific surface area of the NS-GA was obtained by the Brunauer–Emmett–Teller (BET) method, and the pore size distribution was calculated by the Barrett–Joyner–Halenda (BJH) model.

Electrochemical characterization

The electrochemical performances of the samples were tested in symmetric coin cells using a two-electrode system with the cellulosic separator NKK TF 4030 as a separator in the $EMIMBF_4$ electrolyte. The 85% active materials (NS-GA), 15% acetylene black, and 5% polytetrafluoroethylene (PTFE) were mixed in ethanol. Then the mixture was ultrasonicated for about 60 min to obtain a homogenous slurry. Finally, the slurry was pasted into the nickel foam and then the as-prepared nickel foam was dried at 110 °C for 12 h in a vacuum oven. After that, the material-loaded nickel foam was pressed at 10 MPa, with a loading mass of 1.5–2 mg. Then, the prepared electrodes were assembled into button cells in a glove box under an argon atmosphere. The cyclic voltammetry (CV), electrochemical

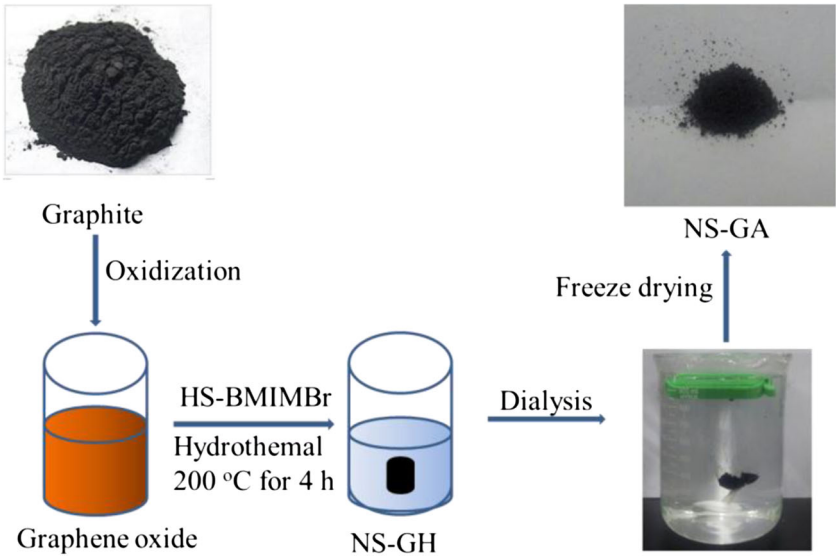

Scheme 1 Schematic illustration of the preparation of the graphene aerogel (NS-GA)

impedance spectroscopy (EIS), and galvanostatic charge/discharge (GCD) were carried out on a CHI660D electrochemical working station (Shanghai, Chenhua Instrument Co., Ltd., China). And the cycle life test was conducted on a CT2001A battery test system (Lanhe, Wuhan, China). The specific capacitance of the active material for the single electrode (C_s, F g^{-1}) and the cell (C_{cell}, F g^{-1}) was calculated from GCD curves by the following equations, respectively [28, 31]:

$$C_s = \frac{2I\Delta t}{m\Delta V} \quad (1)$$

$$C_{cell} = \frac{1}{4}C_s \quad (2)$$

where I (A) is the discharge current, Δt (s) is the discharge time, m (g) is the mass of the active material in the single electrode, and ΔV (V) is the change in cell potential corrected from the ohmic drop.

Base on the specific capacitance, the energy density (E, Wh kg^{-1}) and power density (P, W kg^{-1}) of the active material for the cell were determined according to the following equations, respectively [32]:

$$E = \frac{1}{7.2}C_{cell}\Delta V^2 \quad (3)$$

$$P = 3600\frac{E}{\Delta t} \quad (4)$$

Results and discussion

Characterization of the materials

The morphology of the NS-GA was investigated by SEM and TEM. As displayed in Fig. 1a, the obtained NS-GA appears an interconnected hierarchical porous structure, and such porous structure is essential for accelerating the transfer of electrons and transport of electrolyte ions. Besides, the interconnected network porous structure is loose, and thus can provide a passable channel for the migration of ions/charges. Remarkably, the TEM image (Fig. 1b) of the NS-GA shows a straticulate morphology, indicating that the NS-GA has a graphene-like thin layer structure. Moreover, the NS-GA has wrinkled and folded transparent textures, and no obvious aggregation is clearly observed, which is because the doping of heteroatoms alters the electronic properties of graphene sheets. This pleated texture can supply a larger accessible area for the charge accumulation. And the unique porous structure of the NS-GA is effective to prevent the aggregation of graphene sheets by the π-π conjugation and electrostatic interactions between the graphene sheets and the imidazole rings.

N_2 adsorption–desorption isotherm was measured to deeply investigate the porous nature of the NS-GA. Figure 2a displays a type IV isotherm according to IUPAC classification, indicating the existence of mesoporous structures [33]. The BET specific surface area of the NS-GA is 94.25 m^2 g^{-1}, and its pore volume is 0.51 cm^3 g^{-1}. Besides, there is an H3-type hysteresis loop in the middle pressure (P/P_0 = 0.46–0.99) range, indicating that the NS-GA possesses a heterogeneous porous structure between graphene layers. Figure 2b shows the pore size distribution of the NS-GA analyzed by the BJH model. Obviously, there are two main distributions centered at 35 nm and 125 nm, respectively, confirming that the NS-GA is a typical hierarchical pore characteristic. The macropores can be used as a reservoir for ion-buffering, and the mesopores can efficiently ensure the transport of electrons and ions [34]. The hierarchical porous structure of the NS-GA can offer more accessible sites for electrolyte ions and then increase the capacitance performance.

X-ray photoelectron spectroscopy (XPS) was used to demonstrate the elemental compositions and bonding

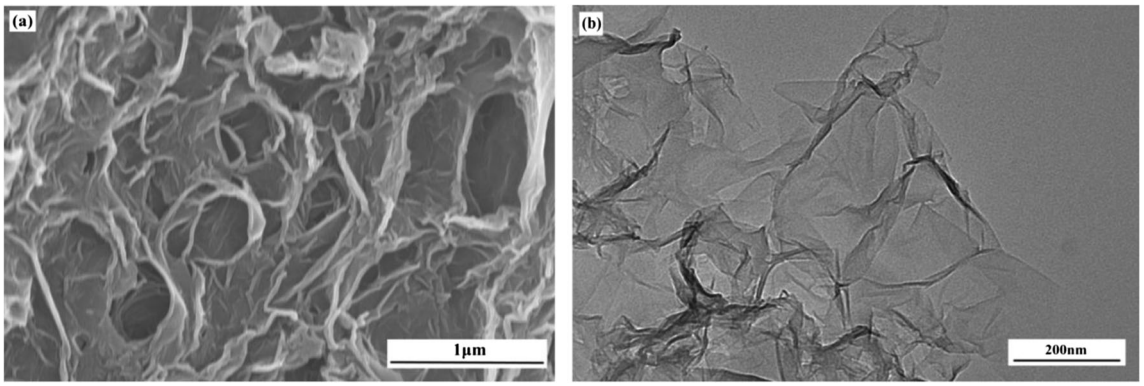

Fig. 1 FESEM (**a**) and TEM (**b**) images of the NS-GA

configurations of the NS-GA. As shown in Fig. 3a, five peaks at 285.3 eV, 407.1 eV, 534.2 eV, 228.0 eV, and 164.1 eV are attributed respectively to C1s, N1 s, O1s, S2 s, and S2p, suggesting that the nitrogen and sulfur atoms were doped successfully into the NS-GA. And, the atomic percentages are summarized in Table 1. The high-resolution spectrum of C1s (Fig. 3b) can be deconvoluted into four peaks at 284.9 eV, 285.4 eV, 286.7 eV, and 291.0 eV referring to C=C/C–C, C–N/C–S, C=O, and O–C=O, respectively [34, 35]. The N1s spectrum (Fig. 3c) can be deconvoluted into two peaks with a binding energy of 397.6 eV and 402.0 eV, corresponding to pyridinic N and oxidized N, respectively [36]. The negatively charged pyridinic N atoms are located at the edges of graphene sheets, which provide abundantly accessible defects of graphene for charge storage [37], and thus enhance the electrochemical performance of the materials. Figure 3d shows the S2p high-resolution spectrum which can be observed two obvious peaks at 164.5 eV and 165.3 eV, corresponding respectively to S2p3/2 and S2p1/2 of the thiophene-S (–C–S–C–) arising from spin-orbit coupling [38]. The sulfur dopant species, such as thiophenic sulfur and sulfone, play a significant role in modifying the surface properties of carbon materials [39]. The doping of sulfur atoms is due to the reactions of –SH groups on HS-BMIMBr with oxygen-containing functional groups on the surface of GO.

The crystal structures of the prepared NS-GA, GA, and GO were measured by XRD. Figure 4a shows the corresponding XRD patterns. The diffraction peak of GO at $2\theta = 10.9°$ can be attributed to the (002) crystalline plane, and the layer spacing of 0.81 nm indicates that graphite was converted to graphene oxide. For NS-GA and GA, the peak at $2\theta = 10.9°$ entirely disappeared, and a broad diffraction peak centered at about 25° appeared, indicating that the GO had been reduced to graphene (rGO). Furthermore, the diffraction peak of the NS-GA was broader and weaker than that of GA, meaning that the NS-GA was of typical amorphous graphitic feature [40] and the defects were formed due to the doping of N and S atoms. The interlayer spacings of rGO sheets in the NS-GA and GA are 0.37 nm and 0.35 nm, respectively. And the interactions between rGO sheets and HS-BMIMBr enlarge the layer spacing and provide more passable channels for the transport of ions.

Raman spectroscopy can be used to characterize the microstructure of carbonaceous materials. As shown in Fig. 4b, typical peaks of the as-prepared materials are centered at 1340 cm^{-1} and 1589 cm^{-1} which are called as D band and G band, respectively. The D band is associated with structural defects and partially disordered structures of graphene materials, and the G band is related to in-plane stretching vibration of sp^2 C–C bonds [41]. In general, the intensity ratio of D and G peak (I_D/I_G)

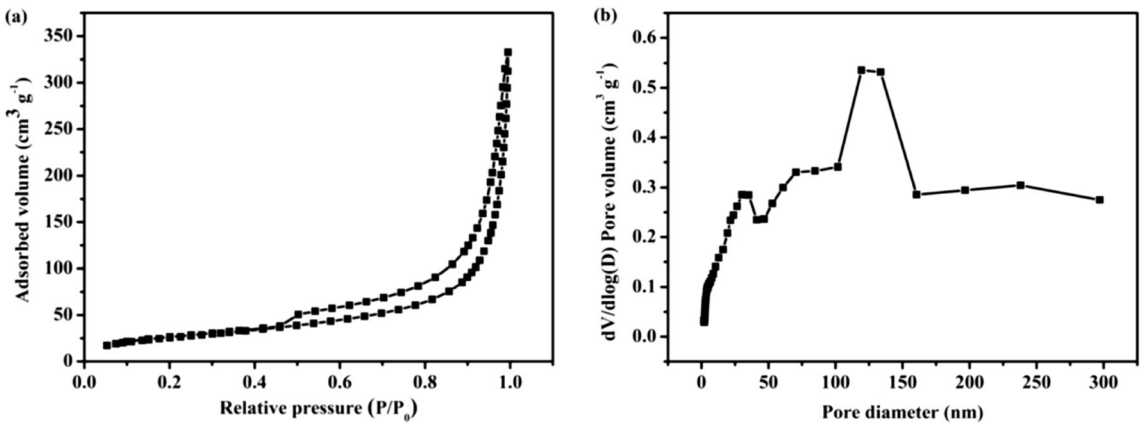

Fig. 2 Nitrogen adsorption–desorption isotherm of the NS-GA (**a**) and BJH adsorption pore size distribution (**b**)

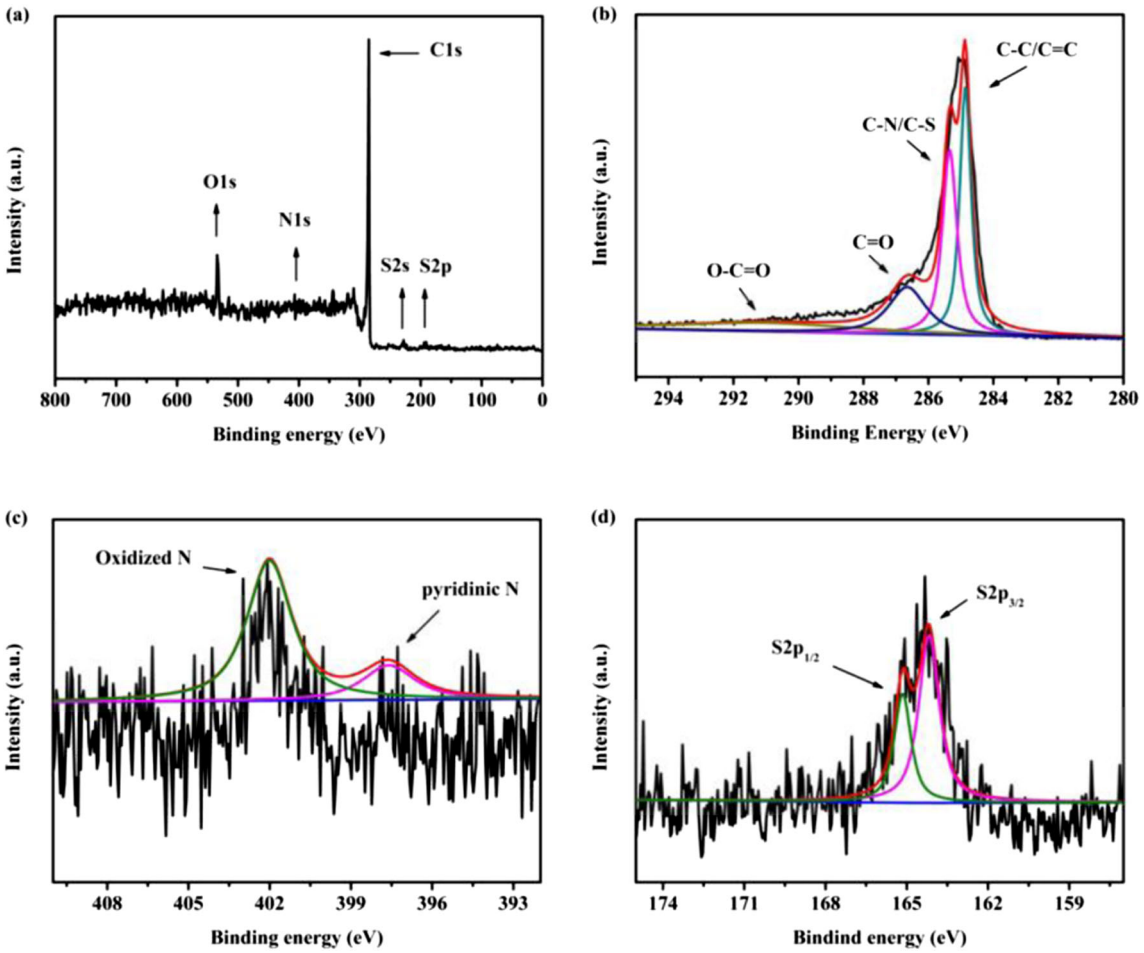

Fig. 3 Full XPS spectrum of NS-GA (**a**); high-resolution spectra of C1s (**b**), N1s (**c**), and S2p (**d**) of NS-GA

reflects the disorder degree of graphene materials. The values of I_D/I_G for GO and NS-GA are 0.95 and 1.27, respectively, indicating that the doping of N and S generates a large number of defects and imperfections in the carbon lattice.

Electrochemical performances of the samples

The electrochemical properties of the supercapacitors based on NS-GA and GA were investigated in the two-electrode system using $EMIMBF_4$ as the electrolyte. As shown in Fig. 5a, the NS-GA electrode presents an approximately rectangular CV shape similar to that of GA at a scan rate of 200 mV s^{-1}, illustrating that the main energy storage mode of the NS-GA and GA is electric double layer capacitance. Furthermore, the CV curve area of the NS-GA is larger than that of GA, meaning that the NS-GA owns higher specific capacitance. A comparison of GCD curves for NS-GA and GA is shown in Fig. 5b at a current density of 2 A g^{-1}. The two curves appear an almost symmetrical triangular shape, manifesting that both NS-GA and GA have good capacitance performance, and the NS-GA electrode has longer charge and discharge time than the GA. Figure 5c presents their good rate capability. The NS-GA displays a specific capacitance of 182.3 F g^{-1} at a current density of 1 A g^{-1}, while the specific capacitance of pure GA is 117.2 F g^{-1}. The specific capacitance of the NS-GA still retains 127.0 F g^{-1} at a high current density of 10 A g^{-1} with capacitance retention of 70%, indicating that the NS-GA has a good capacitance performance and rate capability.

Table 1 Atomic percentage of C, O, N, and S in the NS-GA

Sample	C (at%)	O (at%)	N (at%)	S (at%)
NS-GA	85.68	10.13	2.89	1.31

EIS measurements were conducted in the range from 1 to 100 kHz at a 5-mV amplitude, and the Nyquist plots are shown in Fig. 5d. The plots can be divided into three parts, including the intercept of the curve at high frequencies from the *x*-axis which provides information on the series resistance (R_s), incomplete semicircle in the high-frequency region representing the charge transfer resistance (R_{ct}), and vertical line in the low frequency corresponding to the ion diffusion resistance [42–44]. The R_s values of the NS-GA and GA are 1.3 and 3.1 Ω,

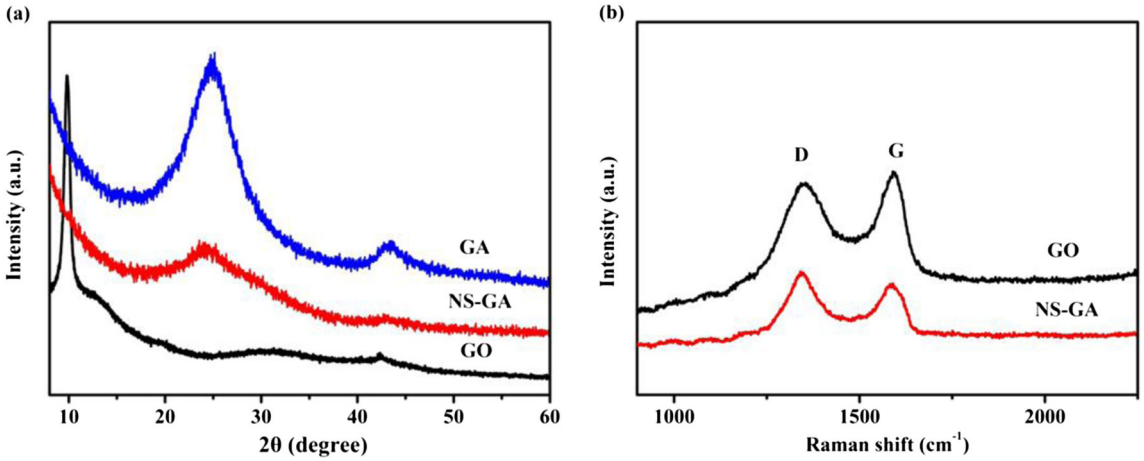

Fig. 4 XRD patterns (**a**) and Raman spectra (**b**) of the samples

respectively, proving that the NS-GA has lower internal resistance. The very small diameter of the semicircles in the high-frequency region indicates very low charge transfer resistance from electrode materials to the electrolyte. The slope of the vertical line for NS-GA is very high in the low-frequency region, suggesting that there is fast ion diffusion in the electrolyte to the surface of the NS-GA electrode. The lower resistance of the NS-GA was related to the uniquely interconnected porous structure and the co-doping of heteroatoms which promote the diffusion of ions and increase the interfacial wettability between the electrode surface and the electrolyte.

Figure 6a shows the CV curves of the NS-GA at scan rates from 5 to 200 mV s^{-1} with the voltage range of 0–4 V. The CV curves display a nearly rectangular shape, indicating that the

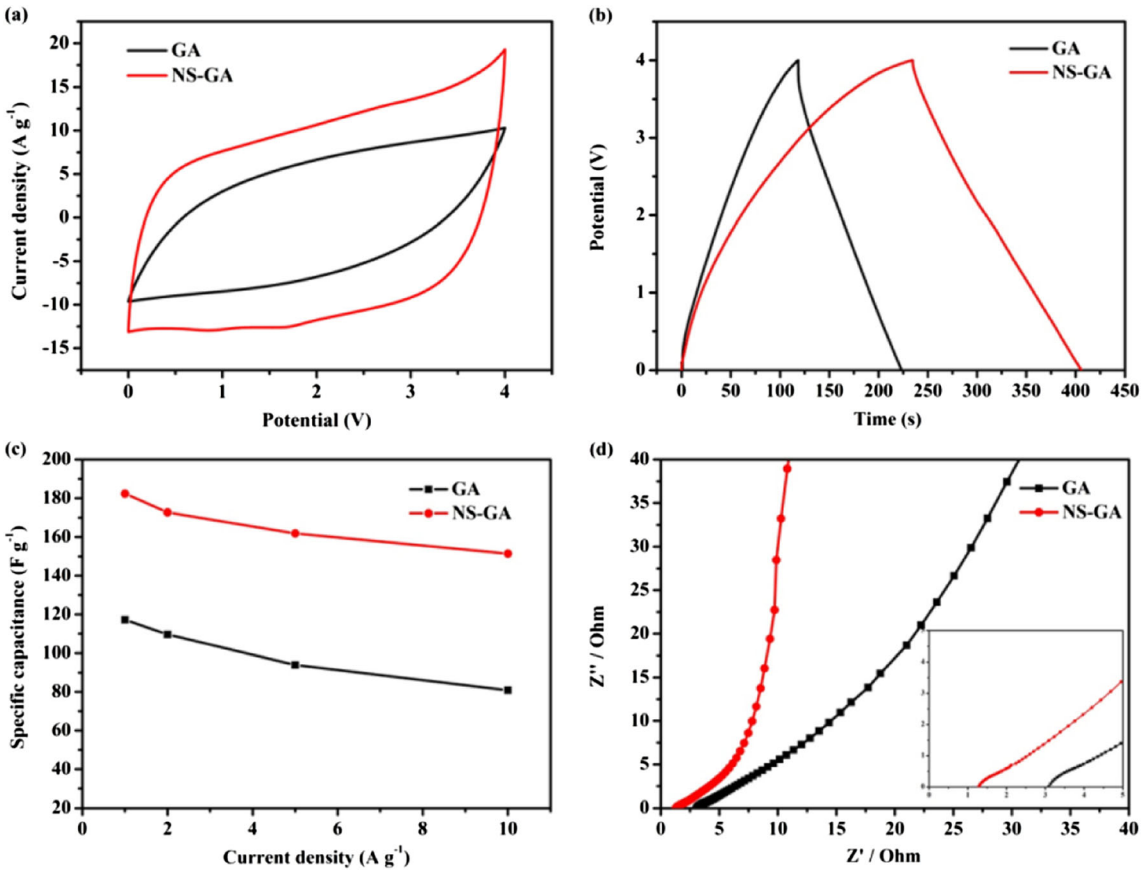

Fig. 5 Electrochemical performances of NS-GA and GA electrodes using ionic liquid $EMIMBF_4$ electrolyte in the two-electrode system: **a** CV curves at a scan rate of 200 mV s^{-1}; **b** GCD curves at a current density of 2 A g^{-1}; **c** Specific capacitance at different current density; **d** Nyquist plots and the inset is the amplification at high-frequency range

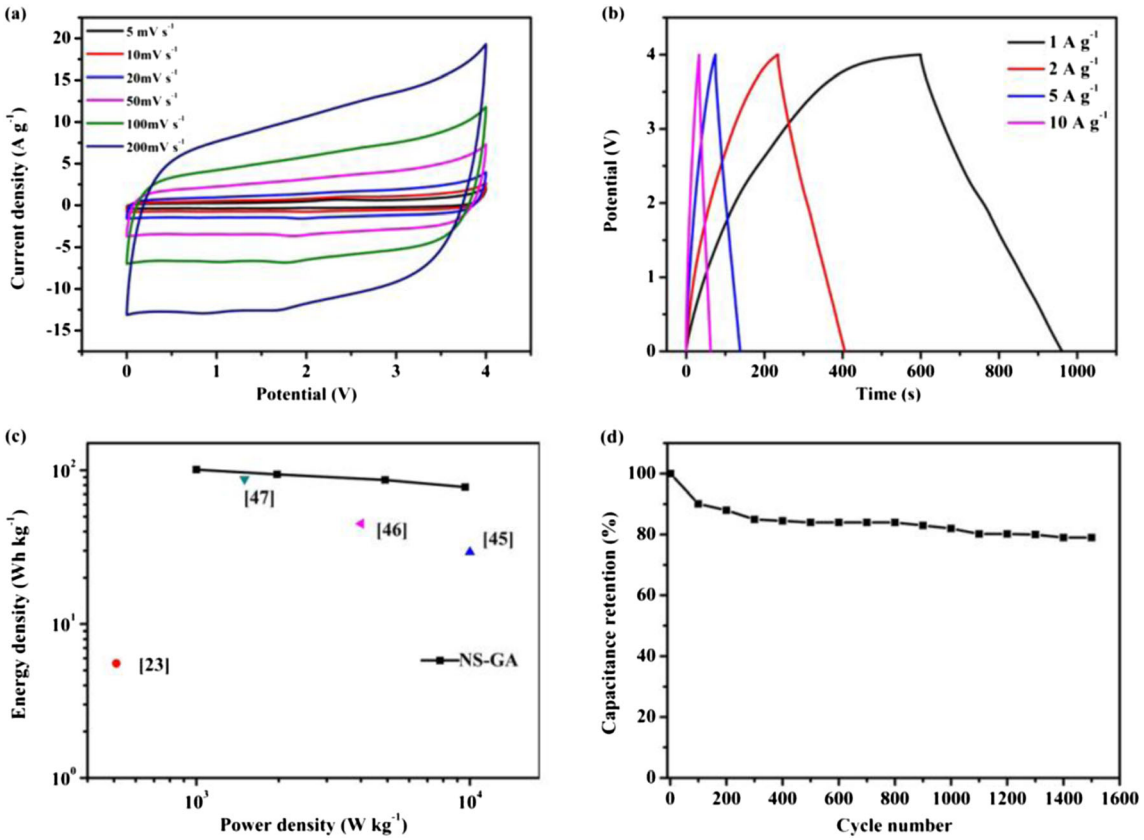

Fig. 6 **a** CV curves of NS-GA at various scan rates; **b** GCD curves at different current densities; **c** Ragone plot of NS-GA electrode compared with other previously reported cells [23, 45–47]; and **d** Cyclic stability test of NS-GA for 1500 cycles at a current density of 1 A g^{-1}

main energy storage mechanism is an ideal electric double layer capacitance. Even though at a high scan rate of 200 mV s^{-1}, the CV curve of the NS-GA still holds a good rectangular shape, revealing that the NS-GA has good capacitive behaviors. The slight asymmetry suggests that there is pseudocapacitance behavior caused by the doping of heteroatoms [48]. The GCD profiles of the NS-GA at different current densities from 1 to 10 A g^{-1} are shown in Fig. 6b. It is obvious that the GCD curves for the NS-GA show an imperfect symmetric triangular form, which suggests that the significant capacitance contribution results from electric double layer capacitance [34] and relatively little pseudocapacitance. The conclusion from GCD profiles is consistent with that from the CV curves.

The energy density is one of the important criteria which decide the practical utility of supercapacitors. The Ragone plot for the NS-GA-based supercapacitor is shown in Fig. 6c. The NS-GA material exhibits a high energy density of 101 Wh kg^{-1} at a power density of 1 kW kg^{-1}, which was superior to those of previously reported carbon materials with the same or different electrolytes, as shown in Table 2. Moreover, as the power density increases, the energy density

Table 2 Comparison of energy density and power density of various carbon materials

Samples	Electrolyte	Electrode system	Energy density (Wh kg^{-1})	Power density (kW kg^{-1})	Reference
N, S co-doped porous carbon nanosheets	1 M Na_2SO_4	2	21.00	0.18	[49]
N, S co-doped hole defect graphene hydrogel	PVA/H_2SO_4	2	14.80	5.20	[50]
Fluorinated graphene hydrogels-150	6 M KOH	2	5.55	0.51	[45]
N, S co-doped graphene	6 M KOH	2	29.40	10.00	[46]
Carbon nanotubes-2900	$EMIMBF_4$	2	45	4.0	[47]
Hierarchical porous carbon spheres/graphene	$BMIMBF_4$	2	87.50	1.50	[23]
S, P co-doped activated graphene aerogel	$BMIMPF_6$	3	88.50	5.30	[41]
N, S co-doped graphene aerogel	$EMIMBF_4$	2	101.00	1.00	This work

decreases slightly, indicating that the NS-GA has excellent rate capability. The cycling stability of the NS-GA was investigated by galvanostatic charge/discharge at a current density of 1 A g^{-1} (Fig. 6d). The capacitor retention rate was 80% after charging-discharging for 1500 cycles.

Conclusions

In general, nitrogen and sulfur co-doped graphene aerogel (NS-GA) with hierarchical porous structure was successfully prepared using HS-BMIMBr via a simple and convenient one-step hydrothermal method. The incorporation of heteroatoms into the graphene materials made the prepared NS-GA have a large number of pore structures. These hierarchical porous structures provide more channels for the rapid migration of electrolyte ions, and thus promote the diffusion of ions. The as-prepared NS-GA used as the electrode material exhibits a high specific capacitance of 182.3 F g^{-1} at 1 A g^{-1}, excellent rate performance, and good cycling stability. More importantly, the NS-GA shows an energy density of 101 Wh kg^{-1} at a power density of 1 kW kg^{-1} in the $EMIMBF_4$ electrolyte. The NS-GA is a potential electrode material for high-performance supercapacitors.

Funding information This work was financially supported by the National Natural Science Foundation of China (Nos. 21573058, 21303044, and 21173070) and Program for Innovative Research Team in Science and Technology in University of Henan Province (15IRTSTHN 003, 17IRTSTHN 001).

References

1. Zhao Y, Liu M, Deng X, Miao L, Tripathi PK, Ma X, Zhu D, Xu Z, Hao Z, Gan L (2015) Nitrogen-functionalized microporous carbon nanoparticles for high performance supercapacitor electrode. Electrochim Acta 153:448–455
2. Yin Y, Li R, Li Z, Liu J, Gu Z, Wang G (2014) A facile self-template strategy to fabricate three-dimensional nitrogen-doped hierarchical porous carbon/graphene for conductive agent-free supercapacitors with excellent electrochemical performance. Electrochim Acta 125(12):330–337
3. Zhang L, Zhu Y, Zhao W, Zhang L, Ye X, Feng J-J (2018) Facile one-step synthesis of three-dimensional freestanding hierarchical porous carbon for high energy density supercapacitors in organic electrolyte. J Electroanal Chem 818:51–57
4. Xiao X, Wang G, Zhang M, Wang Z, Zhao R, Wang Y (2017) Electrochemical performance of mesoporous ZnCo2O4 nanosheets as an electrode material for supercapacitor. Ionics 24(8):2435–2443
5. Zhang D, Zheng L, Ma Y, Lei L, Li Q, Li Y, Luo H, Feng H, Hao Y (2015) Synthesis of nitrogen- and sulfur-codoped 3D cubic-ordered mesoporous carbon with superior performance in supercapacitors. ACS Appl Mater Interfaces 6(4):2657–2665
6. Uppugalla S, Male U, Srinivasan P (2014) Design and synthesis of heteroatoms doped carbon/polyaniline hybrid material for high performance electrode in supercapacitor application. Electrochim Acta 146:242–248
7. Chen C, Fan W, Ma T, Fu X (2014) Fabrication of functionalized nitrogen-doped graphene for supercapacitor electrodes. Ionics 20(10):1489–1494
8. Zhu Y, Murali S, Cai W, Li X, Ji WS, Potts JR, Ruoff RS (2010) Graphene-based materials: graphene and graphene oxide: synthesis, properties, and applications. Adv Mater 22(35):3906–3924
9. Xu Y, Lin Z, Huang X, Wang Y, Huang Y, Duan X (2013) Functionalized graphene hydrogel-based high-performance supercapacitors. Adv Mater 25(40):5779–5784
10. Sun Y, Wu Q, Shi G (2011) Graphene based new energy materials. Energy Environ Sci 4(4):1113–1132
11. Jiang H, Lee PS, Li C (2012) 3D carbon based nanostructures for advanced supercapacitors. Energy Environ Sci 6(1):41–53
12. Shi YC, Wang AJ, Wu XL, Chen JR, Feng JJ (2016) Green-assembly of three-dimensional porous graphene hydrogels for efficient removal of organic dyes. J Colloid Interface Sci 484:254–262
13. Chmiola J, Yushin G, Gogotsi Y, Portet C, Simon P, Taberna PL (2006) Anomalous increase in carbon capacitance at pore sizes less than 1 nanometer. Science 313(5794):1760–1763
14. Huang J, Sumpter BG, Meunier V (2008) Theoretical model for nanoporous carbon supercapacitors. Angew Chem Int Ed 47(3):520–524
15. Guo DC, Mi J, Hao GP, Dong W, Xiong G, Li WC, Lu AH (2013) Ionic liquid C16mimBF4 assisted synthesis of poly(benzoxazine-co-resol)-based hierarchically porous carbons with superior performance in supercapacitors. Energy Environ Sci 6(2):652–659
16. Wen Z, Wang X, Mao S, Bo Z, Kim H, Cui S, Lu G, Feng X, Chen J (2012) Crumpled nitrogen-doped graphene nanosheets with ultrahigh pore volume for high-performance supercapacitor. Adv Mater 24(41):5610–5616
17. Zhou M, Li X, Cui J, Liu T, Cai T, Zhang H, Guan S (2012) Synthesis and capacitive performances of graphene/N-doping porous carbon composite with high nitrogen content and two-dimensional nanoarchitecture. Int J Electrochem Sci 7(10):9984–9996
18. Fulvio PF, Lee JS, Mayes RT, Wang X, Mahurin SM, Dai S (2011) Boron and nitrogen-rich carbons from ionic liquid precursors with tailorable surface properties. Phys Chem Chem Phys 13(30):13486–13491
19. Wang S, Iyyamperumal E, Roy A, Xue Y, Yu D, Dai L (2011) Vertically aligned BCN nanotubes as efficient metal-free electrocatalysts for the oxygen reduction reaction: a synergetic effect by co-doping with boron and nitrogen. Angew Chem 123(49):11960–11964
20. Hulicova-Jurcakova D, Seredych M, Lu GQ, Kodiweera NK, Stallworth PE, Greenbaum S, Bandosz TJ (2009) Effect of surface phosphorus functionalities of activated carbons containing oxygen and nitrogen on electrochemical capacitance. Carbon 47(6):1576–1584
21. Heintz A (2005) Recent developments in thermodynamics and thermophysics of non-aqueous mixtures containing ionic liquids. A review. J Chem Thermodyn 37(6):525–535
22. Watanabe M, Thomas ML, Zhang S, Ueno K, Yasuda T, Dokko K (2017) Application of ionic liquids to energy storage and conversion materials and devices. Chem Rev 117(10):7190–7239
23. Zhang N, Gao N, Fu C, Liu D, Li S, Jiang L, Zhou H, Kuang Y (2017) Hierarchical porous carbon spheres/graphene composite for supercapacitor with both aqueous solution and ionic liquid. Electrochim Acta 235:340–347
24. Han HB, Zhou SS, Zhang DJ, Feng SW, Li LF, Liu K, Feng WF, Nie J, Li H, Huang XJ (2011) Lithium bis(fluorosulfonyl)imide (LiFSI) as conducting salt for nonaqueous liquid electrolytes for lithium-ion batteries: physicochemical and electrochemical properties. J Power Sources 196(7):3623–3632

25. Lu Z, Chen Y, Liu Z, Li A, Sun D, Zhuo K (2018) Nitrogen and sulfur co-doped graphene aerogel for high performance supercapacitors. RSC Adv 8:18966–18971
26. He C, Sun S, Peng H, Chi PT, Shi D, Xie X, Yang Y (2016) Poly(ionic liquid)-assisted reduction of graphene oxide to achieve high-performance composite electrodes. Compos Part B 106:81–87
27. Jr WSH, Offeman RE (1958) Preparation of graphitic oxide. J Am Chem Soc 80(6):1339
28. Chen Y, Liu Z, Sun L, Lu Z, Zhuo K (2018) Nitrogen and sulfur co-doped porous graphene aerogel as an efficient electrode material for high performance supercapacitor in ionic liquid electrolyte. J Power Sources 390:215–223
29. Itoh H, Naka K, Chujo Y (2004) Synthesis of gold nanoparticles modified with ionic liquid based on the imidazolium cation. J Am Chem Soc 126(10):3026–3027
30. Zhang H, Ye L, Wang X, Li F, Wang J (2014) Functional dialkylimidazolium-mediated synthesis of silver nanocrystals with sensitive Hg(2+)-sensing and efficient catalysis. Chem Commun 50(20):2565–2568
31. Song B, Zhao J, Wang M, Mullavey J, Zhu Y, Geng Z, Chen D, Ding Y, Moon KS, Liu M (2017) Systematic study on structural and electronic properties of diamine/triamine functionalized graphene networks for supercapacitor application. Nano Energy 31:183–193
32. Feng L, Wang K, Zhang X, Sun X, Li C, Ge X, Ma Y (2018) Flexible solid-state supercapacitors with enhanced performance from hierarchically graphene nanocomposite electrodes and ionic liquid incorporated gel polymer electrolyte. Adv Funct Mater 28(4): 1704463
33. Wang B, Qin Y, Tan W, Tao Y, Kong Y (2017) Smartly designed 3D N-doped mesoporous graphene for high-performance supercapacitor electrodes. Electrochim Acta 241:1–9
34. Li J, Zhang G, Fu C, Deng L, Sun R, Wong CP (2017) Facile preparation of nitrogen/sulfur co-doped and hierarchical porous graphene hydrogel for high-performance electrochemical capacitor. J Power Sources 345:146–155
35. Tian G, Liu L, Meng Q, Cao B (2015) Facile synthesis of laminated graphene for advanced supercapacitor electrode material via simultaneous reduction and N-doping. J Power Sources 274:851–861
36. Li Z, Li Z, Shalchi AB, Tan X, Xu Z, Wang H, Olsen BC, Holt CMB, David M (2012) Carbonized chicken eggshell membranes with 3D architectures as high-performance electrode materials for supercapacitors. Adv Energy Mater 2(4):431–437
37. Tian W, Gao Q, Zhang L, Yang C, Li Z, Tan Y, Qian W, Zhang H (2016) Renewable graphene-like nitrogen-doped carbon nanosheets as supercapacitor electrodes with integrated high energy–power properties. J Mater Chem A 4(22):8690–8699
38. Lee WSV, Mei L, Meng L, Xiao LH, Xue JM (2015) Sulphur-functionalized graphene towards high performance supercapacitor. Nano Energy 12:250–257
39. Zhao X, Zhang Q, Chen CM, Zhang B, Reiche S, Wang A, Zhang T, Schlögl R, Su DS (2012) Aromatic sulfide, sulfoxide, and sulfone mediated mesoporous carbon monolith for use in supercapacitor. Nano Energy 1(4):624–630
40. Zhu T, Zhou J, Li Z, Li S, Si W, Zhuo S (2014) Hierarchical porous and N-doped carbon nanotubes derived from polyaniline for electrode materials in supercapacitors. J Mater Chem A 2(31):12545–12551
41. Yu X, Kang Y, Park HS (2016) Sulfur and phosphorus co-doping of hierarchically porous graphene aerogels for enhancing supercapacitor performance. Carbon 101:49–56
42. Wang JG, Yang Y, Huang ZH, Kang F (2013) A high-performance asymmetric supercapacitor based on carbon and carbon–MnO 2 nanofiber electrodes. Carbon 61(11):190–199
43. Qian W, Sun F, Xu Y, Qiu L, Liu C, Wang S, Yan F (2013) Human hair-derived carbon flakes for electrochemical supercapacitors. Energy Environ Sci 7(1):379–386
44. Wei X, Wan S, Jiang X, Wang Z, Gao S (2015) Peanut-shell-like porous carbon from nitrogen-containing poly-N-phenylethanolamine for high-performance supercapacitor. ACS Appl Mater Interfaces 7(40):22238–22245
45. An H, Li Y, Long P, Gao Y, Qin C, Cao C, Feng Y, Feng W (2016) Hydrothermal preparation of fluorinated graphene hydrogel for high-performance supercapacitors. J Power Sources 312:146–155
46. Wang T, Wang LX, Wu DL, Xia W, Jia DZ (2015) Interaction between nitrogen and sulfur in co-doped graphene and synergetic effect in supercapacitor. Sci Rep 5:9591
47. Coromina HM, Adeniran B, Mokaya R, Walsh DA (2016) Bridging the performance gap between electric double layer capacitors and batteries with high-energy/high-power carbon nanotube-based electrodes. J Mater Chem A 4(38):14586–14594
48. Zhang J, Zhou J, Wang D, Hou L, Gao F (2016) Nitrogen and sulfur codoped porous carbon microsphere: a high performance electrode in supercapacitor. Electrochim Acta 191:933–939
49. Li Y, Wang G, Wei T, Fan Z, Yan P (2016) Nitrogen and sulfur co-doped porous carbon nanosheets derived from willow catkin for supercapacitors. Nano Energy 19:165–175
50. Tran NQ, Kang BK, Woo MH, Yoon DH (2016) Enrichment of pyrrolic nitrogen by hole defects in nitrogen and sulfur co-doped graphene hydrogel for flexible supercapacitors. Chemsuschem 9(16):2261–2268